

Class-G Power Amplifiers

Most types of audio power amplifier are less efficient than Class-B; for example, Class-AB is markedly less efficient at the low end of its power capability, while it is clear from Chapter 10 that Class-A wastes virtually all the energy put into it. Building amplifiers with higher efficiency is more difficult. Class-D, using ultrasonic pulse width modulation, promises high efficiency and indeed delivers it, but it is undeniably a difficult technology, and its linearity is still a long way short of Class-B. The practical efficiency of Class-D rests on details of circuit design and device characteristics. The apparently unavoidable LC output filter – second order at least – can only give a flat response into one load impedance, and its magnetics are neither cheap nor easy to design. There are likely to be some daunting EMC difficulties with emissions. Class-D is not an attractive proposition for high-quality domestic amplifiers that must work with separate speakers of unknown impedance characteristics.

There is, however, the Class-G method. Power is drawn from either high- or low-voltage rails as the signal level demands. This technology has taken a long time to come to fruition, but is now used in very-high-power amplifiers for large PA systems, where the savings in power dissipation are important, and is also making its presence felt in home theater systems; if you have seven or eight power amplifiers instead of two their losses are rather more significant. Class-G is firmly established in powered subwoofers, and even in ADSL telephone-line drivers. Given the current concern for economy in energy consumption, Class-G may well become more popular in mainstream areas where its efficiency can be used as a marketing point. It is a technology whose time has come.

The Principles of Class-G

Music has a large peak-to-mean level ratio. For most of the time the power output is a long way below the peak levels, and this makes possible the improved efficiency of Class-G. Even rudimentary statistics for this ratio for various genres of music are surprisingly hard to find, but it is widely accepted that the range between 10dB for compressed rock and 30dB for classical material covers most circumstances.

If a signal spends most of its time at low power, then while this is true a low-power amplifier will be much more efficient. For most of the time lower output levels are supplied from the lowest-voltage rails, with a low voltage drop between rail and output, and correspondingly low dissipation. The most popular Class-G configurations have two or three pairs of supply rails, two being usual for hi-fi, while three is more common in high-power PA amplifiers.

When the relatively rare high-power peaks do occur they must be handled by some mechanism that can draw high power, causing high internal dissipation, but which only does so for brief periods. These infrequent peaks above the transition level are supplied from the high-voltage pair of rails. Clearly the switching between rails is the heart of the matter, and anyone who has ever done any circuit design will immediately start thinking about how easy or otherwise it will be to make this happen cleanly with a high-current 20 kHz signal.

There are two main ways to arrange the dual-rail system: series and parallel (i.e. shunt). This chapter deals only with the series configuration, as it seems to have had the greatest application to hi-fi. The parallel version is more often used in high-power PA amplifiers.

Introducing Series Class-G

A series configuration Class-G output stage using two rail voltages is shown in Figure 12.1. The so-called inner devices are those that work in Class-B; those that perform the rail-switching on signal peaks are called the outer devices – by me, anyway. In this design study the EF type of output stage is chosen because of its greater robustness against local HF instability, though the CFP configuration could be used instead for inner, outer, or both sets of output devices, given suitable care. For maximum power efficiency the inner stage normally runs in Class-B, though there is absolutely no reason why it could not be run in Class-AB or even Class-A; there will be more discussion of these intriguing possibilities later. If the inner power devices are in Class-B, and the outer ones conduct for much less than 50% of a cycle, being effectively in Class-C, then according to the classification scheme I have proposed^[1], this should be denoted Class-B + C. The plus sign indicates the series rather than shunt connection of the outer and inner power devices. This basic configuration was developed by Hitachi to reduce amplifier heat dissipation^[2,3]. Musical signals spend most of their time at low levels, having a high peak/mean ratio, and power dissipation is greatly reduced by drawing from the lower $\pm V_1$ supply rails at these times.

The inner stage TR3, TR4 operates in normal Class-B. TR1, TR2 are the usual drivers and R1 is their shared emitter resistor. The usual temperature-compensated V_{bias} generator is required, shown here theoretically split in half to maintain circuit symmetry when the stage is SPICE simulated; since the inner power devices work in Class-B it is their temperature that must be tracked to maintain quiescent conditions. Power from the lower supply is drawn through D3 and D4, often called the commutating diodes, to emphasize their rail-switching action. The word ‘commutation’ avoids confusion with the usual Class-B crossover at zero volts. I have called the level at which rail-switching occurs the transition level.

When a positive-going instantaneous signal exceeds low rail + V_1 , D1 conducts, TR5 and TR6 turn on and D3 turns off, so the entire output current is now taken from the high-voltage + V_2 rail, with the voltage drop and hence power dissipation shared between TR4 and TR6. Negative-going signals are handled in exactly the same way. Figure 12.2 shows how the collector voltages of the inner power devices retreat away from the output rail as it approaches the lower supply level.

Class-G is commonly said to have worse linearity than Class-B, the blame usually being loaded onto the diodes and problems with their commutation. As usual, received wisdom is only half of

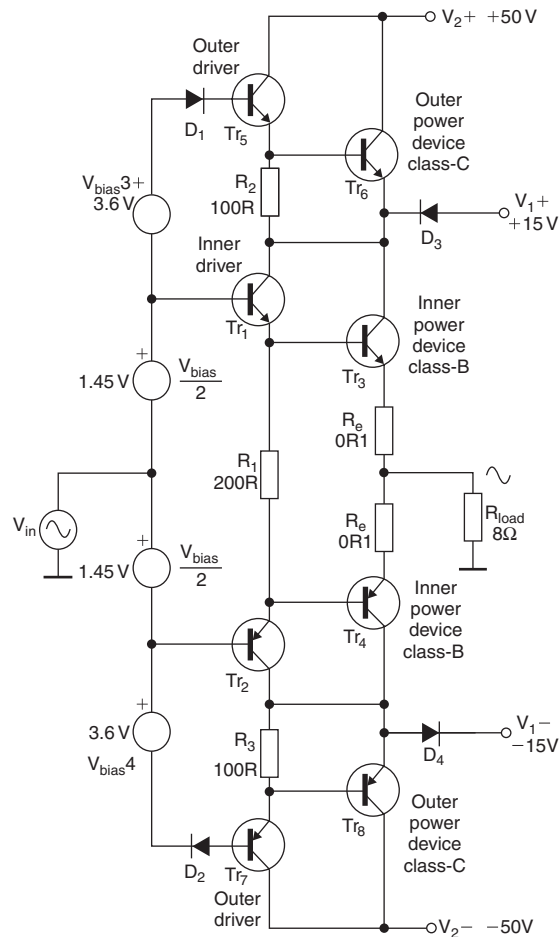


Figure 12.1: A series Class-G output stage, alternatively Class-B + C. Voltages and component values are typical. The inner stage is Class-B EF. Biasing by my method

the story, if that, and there are other linearity problems that are not due to sluggish diodes, as will be revealed shortly. It is inherent in the Class-G principle that if switching glitches do occur they only happen at moderate power or above, and are well displaced away from the critical crossover region where the amplifier spends most of its time. A Class-G amplifier has a low-power region of true Class-B linearity, just as a Class-AB amplifier has a low-power region of true Class-A performance.

Efficiency of Class-G

The standard mathematical derivation of Class-B efficiency with sine-wave drive uses straightforward integration over a half-cycle to calculate internal dissipation against voltage fraction, i.e. the fraction of possible output voltage swing. As is well known, in Class-B the maximum heat dissipation is about 40% of maximum output power, at an output voltage fraction of 63%, which also delivers 40% of the maximum output power to the load.

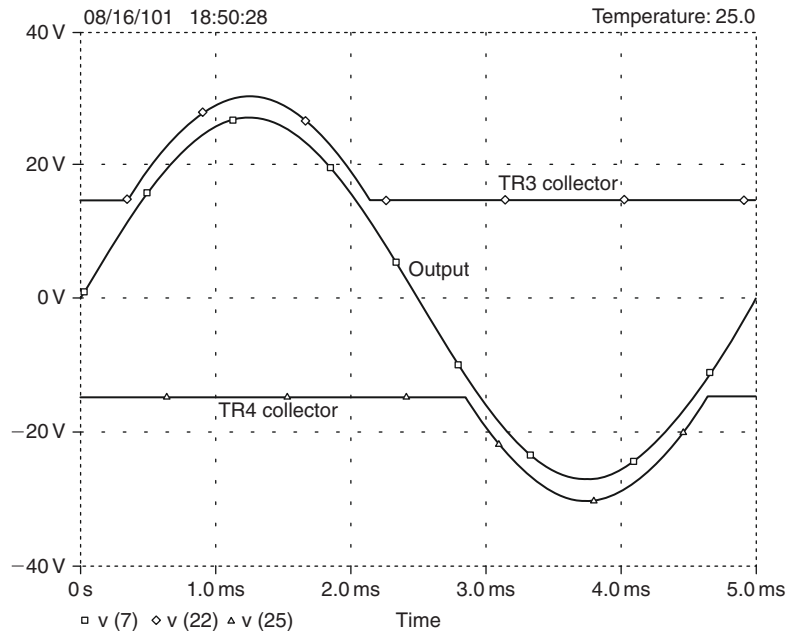


Figure 12.2: The output of a Class-G stage and the voltages on the collectors of the inner output devices

The mathematics is simple because the waveforms do not vary in shape with output level. Every possible idealization is assumed, such as zero quiescent current, no emitter resistors, no $V_{ce(sat)}$ losses and so on. In Class-G, on the other hand, the waveforms are a strong function of output level, requiring variable limits of integration and so on, and it all gets very unwieldy.

The SPICE simulation method described by Self^[4] is much simpler, if somewhat laborious, and can use any input waveform, yielding a Power Partition Diagram (PPD), which shows how the power drawn from the supply is distributed between output device dissipation and useful power in the load.

No one disputes that sine waves are poor simulations of music for this purpose, and their main advantage is that they allow direct comparison with the purely mathematical approach. However, since the whole point of Class-G is power saving, and the waveform used has a strong effect on the results, I have concentrated here on the PPD of an amplifier with real musical signals or, at any rate, their statistical representation. The triangular probability density function (PDF) approach is described in Self^[5].

Figure 12.3 shows the triangular PDF PPD for conventional Class-B EF, while Figure 12.4 is that for Class-G with $\pm V_2 = 50\text{V}$ and $\pm V_1 = 15\text{V}$, i.e. with the ratio of V_1/V_2 set to 30%. The PPD plots power dissipated in all four output devices, the load, and the total drawn from the supply rails. It shows how the input power is partitioned between the load and the output devices. The total sums to slightly less than the input power, the remainder being accounted for as usual by losses in the drivers and Re resistors. Note that in Class-G power dissipation is shared, though not very equally, between the inner and outer devices, and this helps with efficient utilization of the silicon.

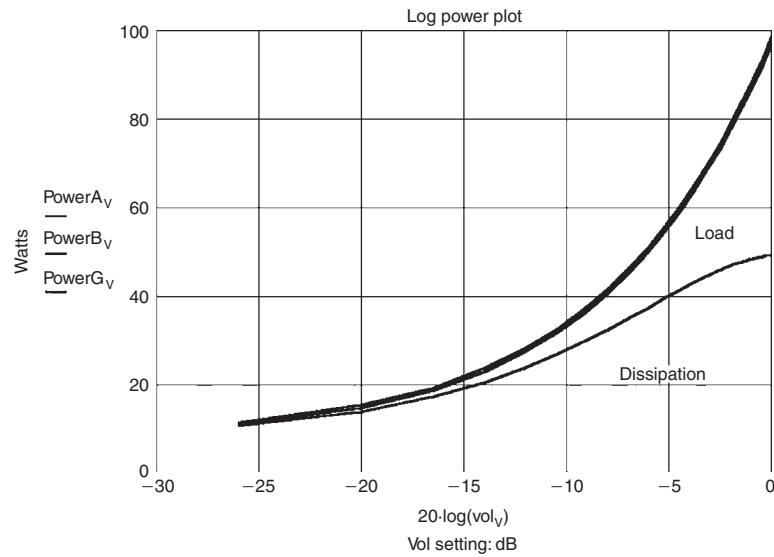


Figure 12.3: Power partition diagram for a conventional Class-B amplifier handling a typical music signal with a triangular probability density function. X-axis is volume

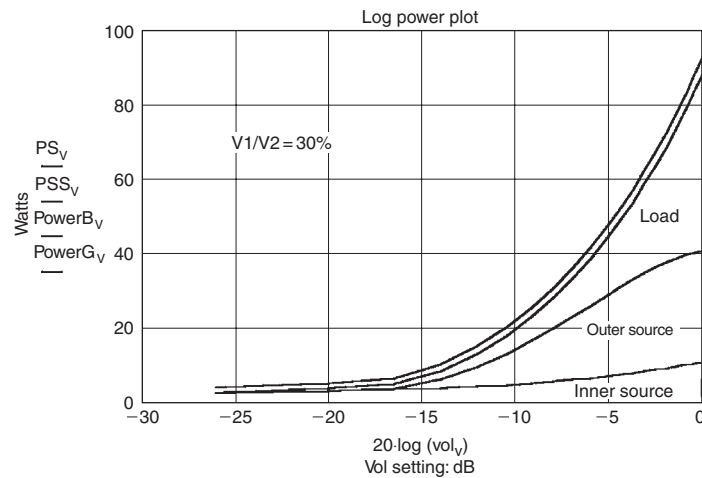


Figure 12.4: Power partition diagram for Class-G with $V1/V2 = 30\%$. Signal has a triangular PDF. X-axis is volume; outer devices dissipate nothing until -15 dB is reached

In Figure 12.4 the lower area represents the power dissipated in the inner devices and the larger area just above represents that in the outer devices; there is only one area for each because in Class-B and Class-G only one side of the amplifier conducts at a time. Outer device dissipation is zero below the rail-switching threshold at -15 dB below maximum output. The total device dissipation at full output power is reduced from 48 W in Class-B to 40 W, which may not appear at first to be a very good return for doubling the power transistors and drivers.

Figure 12.5 shows the same PPD but with $\pm V2 = 50$ V and $\pm V1 = 30$ V, i.e. with $V1/V2$ set to 60%. The low-voltage region now extends up to -6 dB ref. full power, but the inner device

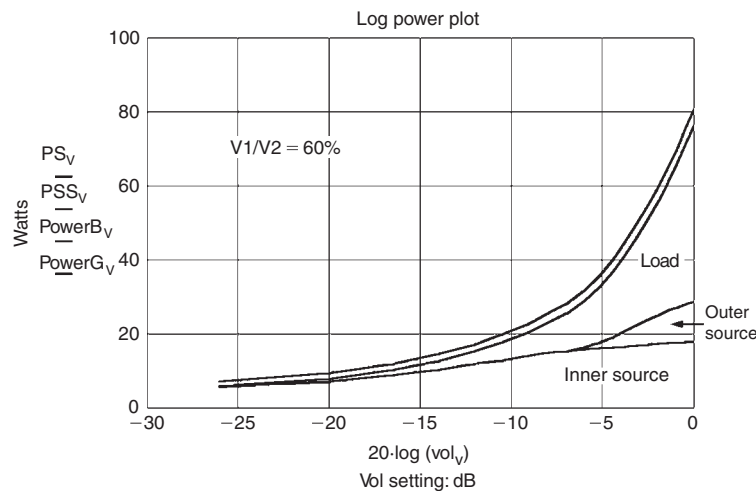


Figure 12.5: Power partition diagram for Class-G with $V1/V2 = 60\%$. Triangular PDF. Compared with Figure 12.4, the inner devices dissipate more and the outer devices almost nothing except at maximum volume

dissipation is higher due to the higher $V1$ rail voltages. The result is that total device power at full output is reduced from 48 W in Class-B to 34 W, which is a definite improvement. The efficiency figure is highly sensitive to the way the ratio of rail voltages compares with the signal characteristics. Domestic hi-fi amplifiers are not operated at full volume all the time, and in real life the lower option for the $V1$ voltage is likely to give lower general dissipation. I do not suggest that $V1/V2 = 30\%$ is the optimum lower-rail voltage for all situations, but it looks about right for most domestic hi-fi.

Practicalities

In my time I have wrestled with many ‘new and improved’ output stages that proved to be anything but. When faced with a new and intriguing possibility, I believe the first thing to do is sketch out a plausible circuit such as Figure 12.1 and see if it works in SPICE simulation. It duly did.

The next stage is to build it, power it from low supply rails to minimize the size of any explosions, and see if it works for real at 1 kHz. This is a bigger step than it looks.

SPICE simulation is incredibly useful but it is not a substitute for testing a real prototype. It is easy to design clever and complex output stages that work beautifully in simulation but in reality prove impossible to stabilize at high frequencies. Some of the more interesting output-triple configurations seem to suffer from this.

The final step – and again it is a bigger one than it appears – is to prove real operation at 20 kHz and above. Again it is perfectly possible to come up with a circuit configuration that either just does not work at 20 kHz, due to limitations on power transistor speeds, or is provoked into oscillation or other misbehavior that is not set off by a 1 kHz testing.

Only when these vital questions are resolved is it time to start considering circuit details, and assessing just how good the amplifier performance is likely to be.

The Biasing Requirements

The output stage bias requirements are more complex than for Class-B. Two extra bias generators V_{bias3} , V_{bias4} are required to make TR6 turn on before TR3 runs out of collector voltage. These extra bias voltages are not critical, but must not fall too low or become much too high. Should these bias voltages be set too low, so the outer devices turn on too late, then the V_{ce} across TR3 becomes too low, and its current sourcing capability is reduced. When evaluating this issue bear in mind the lowest impedance load the amplifier is planned to drive, and the currents this will draw from the output devices. Fixed Zener diodes of normal commercial tolerance are quite accurate and stable enough for setting V_{bias3} and V_{bias4} .

Alternatively, if the bias voltage is set too low, then the outer transistors will turn on too early, and the heat dissipation in the inner power devices becomes greater than it need be for correct operation. The latter case is rather less of a problem so if in doubt this bias should be chosen to be on the high side rather than the low.

The original Hitachi circuit^[1] put Zeners in series with the signal path to the inner drivers to set the output quiescent bias, their voltage being subtracted from the main bias generator, which was set at 10V or so, a much higher voltage than usual (see Figure 12.6). SPICE simulation showed me that the presence of Zener diodes in the forward path to the inner power devices gave poor linearity, which is not exactly a surprise. There is also the problem that the quiescent conditions will be affected by changes in the Zener voltage. The 10V bias generator, if it is the usual V_{be} -multiplier, will have much too high a temperature coefficient for proper thermal tracking.

I therefore rearrange the biasing as in Figure 12.1. The amplifier forward path now goes directly to the inner devices, and the two extra bias voltages are in the path to the outer devices; since these do not control the output directly, the linearity of this path is of lesser importance. The Zeners are out of the forward path and the bias generator can be the standard sort. It must be thermally coupled to the inner power devices; the outer ones have no effect on the quiescent conditions.

The Linearity Issues of Series Class-G

Series Class-G has often had its linearity called into question because of difficulties with supply-rail commutation. Diodes D3, D4 must be power devices capable of handling a dozen amps or more, and conventional silicon rectifier diodes that can handle such currents take a long time to turn off due to their stored charge carriers. This has the following unhappy effect: when the voltage on the cathode of D3 rises above V_1 , the diode tries to turn off abruptly, but its charge carriers sustain a brief but large reverse current as they are swept from its junction. This current is supplied by TR6, attempting as an emitter-follower to keep its emitter up to the right voltage. So far all is well.

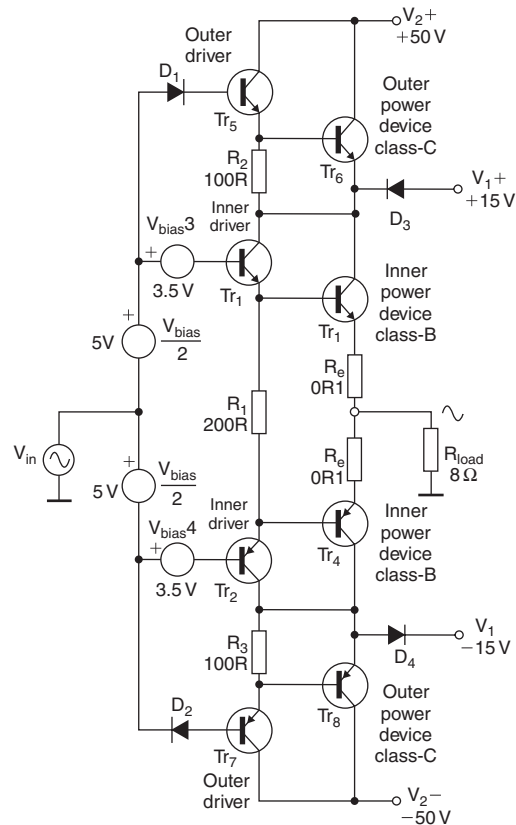


Figure 12.6: The original Hitachi Class-G biasing system, with inner device bias derived by subtracting V_{bias3} , V_{bias4} from the main bias generator

However, when the diode current ceases, TR6 is still conducting heavily, due to its own charge-carrier storage. The extra current it turned on to feed D3 in reverse now goes through the TR3 collector, which accepts it because of TR3's low V_{ce} , and passes it onto the load via TR3 emitter and R_e .

This process is readily demonstrated by a SPICE commutation transient simulation (see Figures 12.7 and 12.8). Note there are only two of these events per cycle – not four, as they only occur when the diodes turn off. In the original Hitachi design this problem was reportedly tackled by using fast transistors and relatively fast gold-doped diodes, but according to Sampei et al.^[2] this was only partially successful.

It is now simple to eradicate this problem. Schottky power diodes are readily available, as they were not in 1976, and are much faster due to their lack of minority carriers and charge storage. They have the added advantage of a low forward voltage drop at large currents of 10A or more. The main snag is a relatively low reverse withstand voltage, but fortunately in Class-G usage the commutating diodes are only exposed at worst to the difference between V_2 and V_1 , and this only when the amplifier is in its low-power domain of operation. Another good point about Schottky power diodes is that they do appear to be robust; I have subjected 50A Motorola devices to 60 A-plus repeatedly without a single failure. This is a good sign. The spikes disappear completely

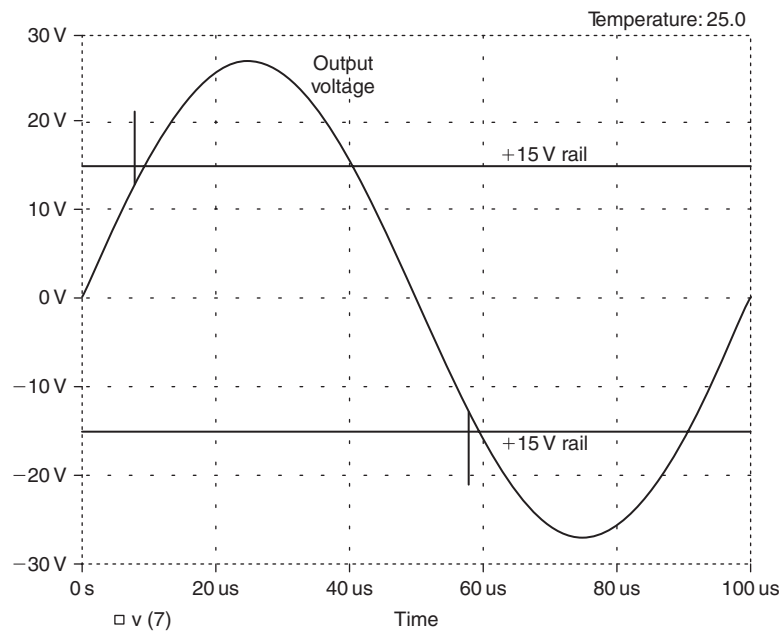


Figure 12.7: Spikes due to charge storage of conventional diodes, simulated at 10 kHz. They only occur when the diodes turn off, so there are only two per cycle. These spikes disappear completely when Schottky diodes are used in the SPICE model

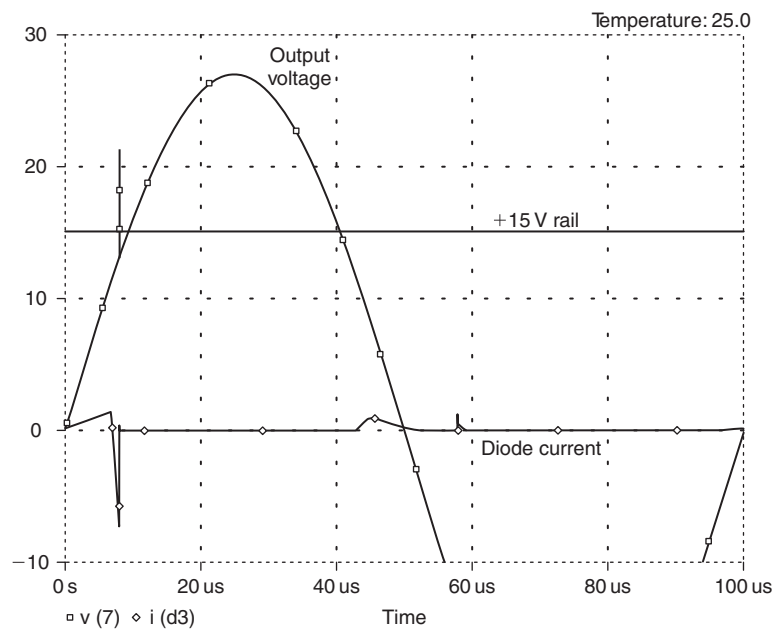


Figure 12.8: A close-up of the diode transient. Diode current rises as output moves away from zero, then reverses abruptly as charge carriers are swept out by reverse-biasing. The spike on the output voltage is aligned with the sudden stop of the diode reverse current

from the SPICE plot if the commutating diodes are Schottky rectifiers. Motorola MBR5025L diodes capable of 50A and 25 PIV were used in simulation.

The Static Linearity

SPICE simulation shows in Figure 12.9 that the static linearity (i.e. that ignoring dynamic effects like diode charge storage) is distinctly poorer than for Class-B. There is the usual Class-B gain wobble around the crossover region, exactly the same size and shape as for conventional Class-B, but also there are now gain-steps at ± 16 V. The result with the inner devices biased into push-pull Class-A is also shown, and proves that the gain-steps are not in any way connected with crossover distortion. Since this is a DC analysis the gain-steps cannot be due to diode-switching speed or other dynamic phenomena, and the Early effect was immediately suspected (the Early effect is the increase in collector current when the collector voltage increases, even though V_{be} remains constant). When unexpected distortion appears in a SPICE simulation of this kind, and effects due to finite transistor beta and associated base currents seem unlikely, a most useful diagnostic technique is to switch off the simulation of the Early effect for each transistor in turn. In SPICE transistor models the Early effect can be totally disabled by setting the parameter VAF to a much higher value than the default of 100, such as 50,000. This experiment demonstrated in short order that the gain-steps were caused wholly by the Early effect acting on both inner drivers and inner output devices. The gain-steps are completely abolished with Early effect disabled. When TR6 begins to act, TR3 V_{ce} is no longer decreasing as the output moves positive, but substantially

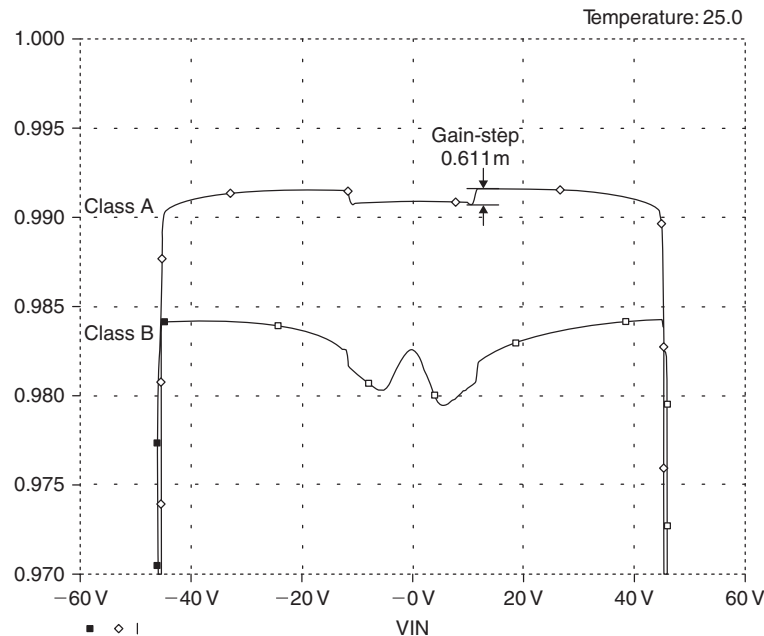


Figure 12.9: SPICE simulation shows variations in the incremental gain of an EF-type Class-G series output stage. The gain-steps at transition (at ± 16 V) are due to Early effect in the transistors. The Class-A trace is the top one, with Class-B optima below. Here the inner driver collectors are connected to the switched inner rails, i.e. the inner power device collectors, as in Figure 12.1

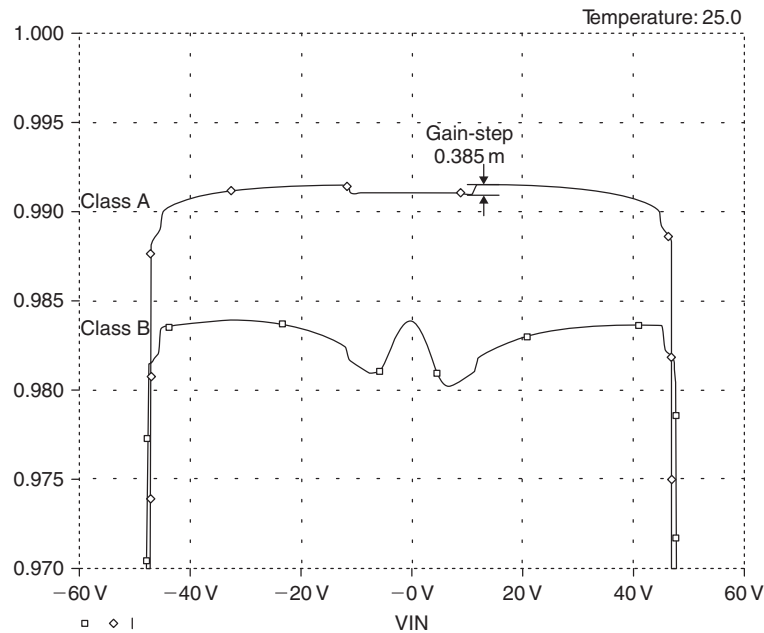


Figure 12.10: Connecting the inner driver collectors to the outer V2 rails reduces Early effect nonlinearities in them, and halves the transition gain-steps

constant as the emitter of Q6 moves upwards at the same rate as the emitter of Q3. This has the effect of a sudden change in gain, which naturally degrades the linearity.

This effect appears to occur in drivers and output devices to the same extent. It can be easily eliminated in the drivers by powering them from the outer rather than the inner supply rails. This prevents the sudden changes in the rate in which driver V_{ce} varies. The improvement in linearity is seen in Figure 12.10, where the gain-steps have been halved in size. The resulting circuit is shown in Figure 12.11. Driver power dissipation is naturally increased by the increased driver V_{ce} , but this is such a small fraction of the power consumed that the overall efficiency is not significantly reduced. It is obviously not practical to apply the same method to the output devices, because then the low-voltage rail would never be used and the amplifier is no longer working in Class-G. The small-signal stages naturally have to work from the outer rails to be able to generate the full voltage swing to drive the output stage.

We have now eliminated the commutating diode glitches and halved the size of the unwanted gain-steps in the output stage. With these improvements made it is practical to proceed with the design of a Class-G amplifier with midband THD below 0.002%.

Practical Class-G Design

The Class-G amplifier design expounded here uses very similar small-signal circuitry to the Blameless Class-B power amplifier, as it is known to generate very little distortion of its own. If the specified supply voltages of ± 50 and ± 15 V are used, the maximum power output is about 120 W into $8\ \Omega$, and the rail-switching transition occurs at 28 W.

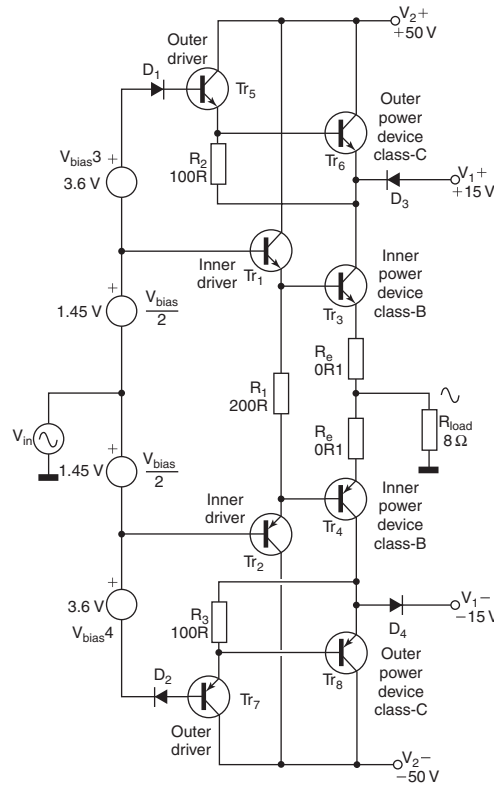


Figure 12.11: A Class-G output stage with the drivers powered from the outer supply rails

This design incorporates various techniques described in this book, and closely follows the Blameless Class-B amp described in Chapter 6, though some features derive from the Trimodal (Chapter 10) and Load-Invariant (Chapter 6) amplifiers. A notable example is the low-noise feedback network, complete with its option of input bootstrapping to give a high impedance when required. Single-slope VI limiting is incorporated for overload protection; this is implemented by Q12, Q13. Figure 12.12 shows the circuit.

As usual in my amplifiers the global NFB factor is a modest 30 dB at 20 kHz.

Controlling Small-Signal Distortion

The distortion from the small-signal stages is kept low by the same methods as for the other amplifier designs in this book, and so this is only dealt with briefly here. The input stage differential pair Q1, Q2 is given local feedback by R5 and R7 to delay the onset of third-harmonic Distortion 1. Internal r_e variations in these devices are minimized by using an unusually high tail current of 6 mA. Q3, Q4 are a degenerated current-mirror that enforces accurate balance of the Q1, Q2 collector currents, preventing the production of second-harmonic distortion. The input resistance ($R3 + R4$) and feedback resistance R16 are made equal and made unusually low, so that base-current mismatches stemming from input device beta variations give a minimal DC offset. V_{be} mismatches in Q1 and Q2 remain, but these are much smaller than the effects of I_b . Even if Q1

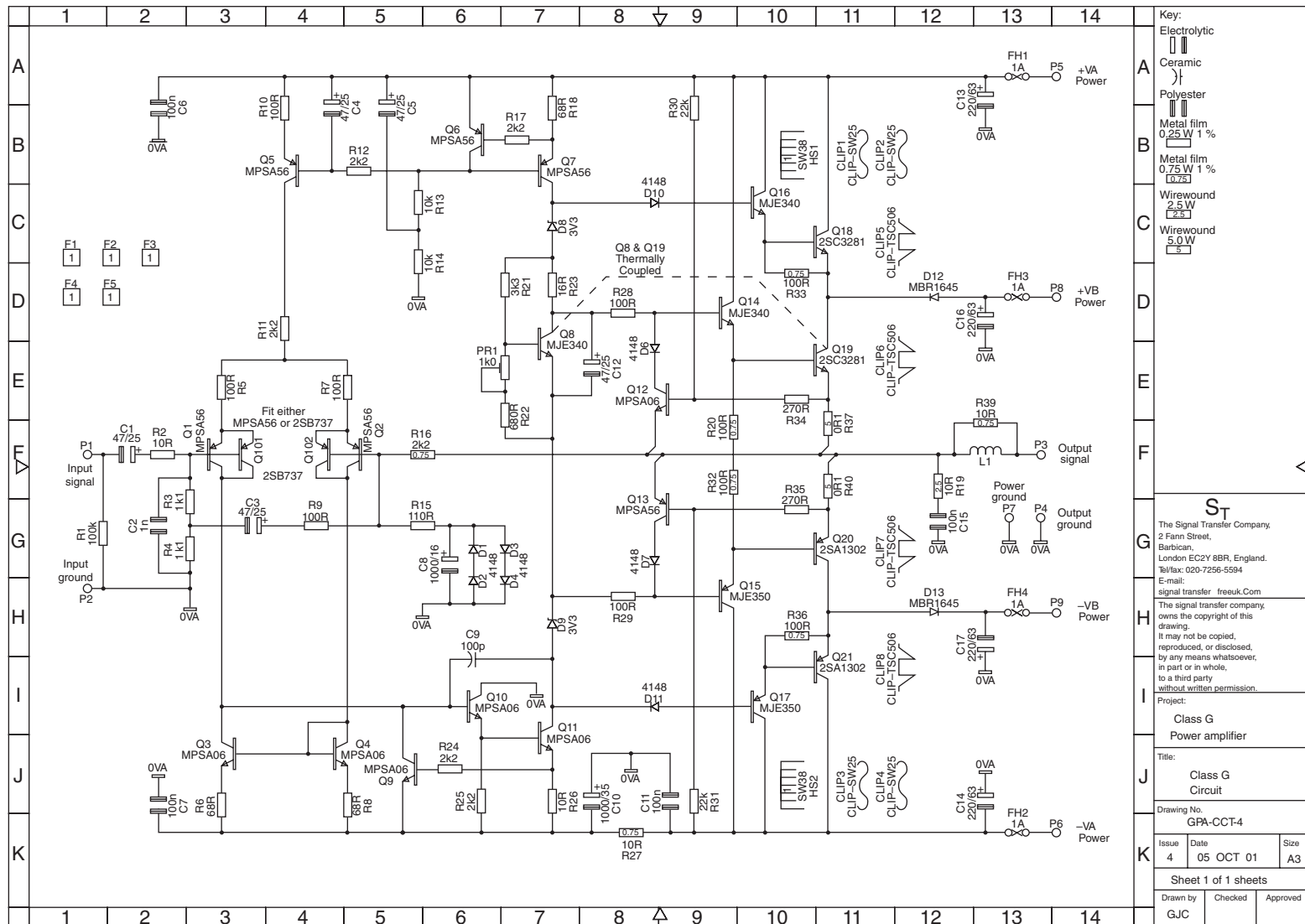


Figure 12.12: The circuit diagram of the Class-G amplifier

and Q2 are high-voltage types with relatively low beta, the DC offset voltage at the output should be kept to less than ± 50 mV. This is adequate for all but the most demanding applications. This low-impedance technique eliminates the need for balance presets or DC servo systems, which is most convenient.

A lower value for R16 implies a proportionally lower value for R15 to keep the gain the same, and this reduction in the total impedance seen by Q2 improves noise performance markedly. However, the low value of R3 plus R4 at 2k2 gives an input impedance that is not high enough for many applications.

There is no problem if the amplifier is to have an additional input stage, such as a balanced line receiver. Proper choice of op-amp will allow the stage to drive a 2k2 load impedance without generating additional distortion. Be aware that adding such a stage – even if it is properly designed and the best available op-amps are used – will degrade the signal-to-noise ratio significantly. This is because the noise generated by the power amplifier itself is so very low – equivalent to the Johnson noise of a resistor of a few hundred ohms – that almost anything you do upstream will degrade it seriously.

If there is no separate input stage then other steps must be taken. What we need at the input of the power amplifier is a low DC resistance, but a high AC resistance; in other words we need either a 50 henry choke or recourse to some form of bootstrapping. There is to my mind no doubt about the way to go here, so bootstrapping it is. The signal at Q2 base is almost exactly the same as the input, so if the mid-point of R3 and R4 is driven by C3, so far as input signals are concerned R3 has a high AC impedance. When I first used this arrangement I had doubts about its high-frequency stability, and so added resistor R9 to give some isolation between the bases of Q1 and Q2. In the event I have had no trouble with instability, and no reports of any from the many constructors of the Trimodal and Load-Invariant designs, which incorporate this option.

The presence of R9 limits the bootstrapping factor, as the signal at the R3–R4 junction is thereby a little smaller than at Q2 base, but it is adequate. With R9 set to 100R, the AC input impedance is raised to 13 k, which should be high enough for almost all purposes. Higher values than this mean that an input buffer stage is required.

The value of C8 shown (1000 μ F) gives an LF roll-off in conjunction with R15 that is -3 dB at 1.4 Hz. The purpose is not impossibly extended sub-bass, but the avoidance of a low-frequency rise in distortion due to nonlinearity effects in C8. If a 100 μ F capacitor is used here the THD at 10 Hz worsens from $<0.0006\%$ to 0.0011%, and I regard this as unacceptable esthetically – if not perhaps audibly. This is not the place to define the low-frequency bandwidth of the system – this must be done earlier in the signal chain, where it can be properly implemented with more accurate non-electrolytic capacitors. The protection diodes D1–D4 prevent damage to C2 if the amplifier suffers a fault that makes it saturate in either direction; it looks like an extremely dubious place to put diodes but since they normally have no AC or DC voltage across them no measurable or detectable distortion is generated.

The voltage-amplifier stage (VAS) Q11 is enhanced by emitter-follower Q10 inside the Miller compensation loop, so that the local negative feedback that linearizes the VAS is increased. This

effectively eliminates VAS nonlinearity. Thus increasing the local feedback also reduces the VAS collector impedance, so a VAS buffer to prevent Distortion 4 (loading of VAS collector by the nonlinear input impedance of the output stage) is not required. Miller capacitor C_{dom} is relatively big at 100 pF, to swamp transistor internal capacitances and circuit strays, and make the design predictable. The slew rate calculates as 40 V/ μ s use in each direction. VAS collector load Q7 is a standard current source.

Almost all the THD from a Blameless amplifier derives from crossover distortion, so keeping the quiescent conditions optimal to minimize this is essential. The bias generator for an EF output stage, whether in Class-B or Class-G, is required to cancel out the V_{be} variations of four junctions in series; those of the two drivers and the two output devices. This sounds difficult, because the dissipation in the two types of devices is quite different, but the problem is easier than it looks. In the EF type of output stage the driver dissipation is almost constant as power output varies, and so the problem is reduced to tracking the two output device junctions. The bias generator Q8 is a standard V_{be} -multiplier, with R23 chosen to minimize variations in the quiescent conditions when the supply rails change. The bias generator should be in contact with the top of one of the inner output devices, and not the heat-sink itself. This position gives much faster and less attenuated thermal feedback to Q8. The VAS collector circuit incorporates not only bias generator Q8 but also the two Zeners D8, D9, which determine how early rail-switching occurs as the inner device emitters approach the inner (lower) voltage rails.

The output stage was selected as an emitter-follower (EF) type as this is known to be less prone to parasitic or local oscillations than the CFP configuration, and since this design was to some extent heading into the unknown it seemed wise to be cautious where possible. R32 is the usual shared emitter resistor for the inner drivers. The outer drivers Q16 and Q17 have their own emitter resistors R33 and R36, which have their usual role of establishing a reasonable current in the drivers as they turn on, to increase driver transconductance, and also in speeding up turn-off of the outer output devices by providing a route for charge carriers to leave the output device bases.

As explained above, the inner driver collectors are connected to the outer rails to minimize the gain-steps caused by the abrupt change in collector voltage when rail transition occurs.

Deciding the size of heat-sink required for this amplifier is not easy, mainly because the heat dissipated by a Class-G amplifier depends very much on the rail voltages chosen and the signal statistics. A Class-B design giving 120 W into $8\ \Omega$ would need a heat-sink with thermal resistance of the order of 1°C/W (per channel); a good starting point for a Class-G version giving the same power would be about half the size, i.e. 2°C/W. The Schottky commutating diodes do not require much heat-sinking, as they conduct only intermittently and have a low forward voltage drop. It is usually convenient to mount them on the main heat-sink, even if this does mean that most of the time they are being heated rather than cooled.

C15 and R38 make up the usual Zobel network. The coil L1, damped by R39, isolates the amplifier from load capacitance. A component with 15–20 turns at 1 inch diameter should work well; the value of inductance for stability is not all that critical.

The Performance

Figure 12.13 shows the THD at 20W and 50W (into 8Ω) and I think this demonstrates at once that the design is a practical competitor for Class-B amplifiers. Compare these results with the upper trace of Figure 12.14, taken from a Blameless Class-B amplifier at 50W, 8Ω . Note the lower trace of Figure 12.14 is for 30kHz bandwidth, used to demonstrate the lack of distortion below 1 kHz; the THD data above 30kHz is in this case meaningless as all the harmonics are filtered out. All the Class-G plots here are taken at 80kHz to make sure any high-order glitching is properly measured.

Figure 12.15 shows the actual THD residual at 50W output power. The glitches from the gain-steps are more jagged than the crossover disturbances, as would be expected from the output stage gain

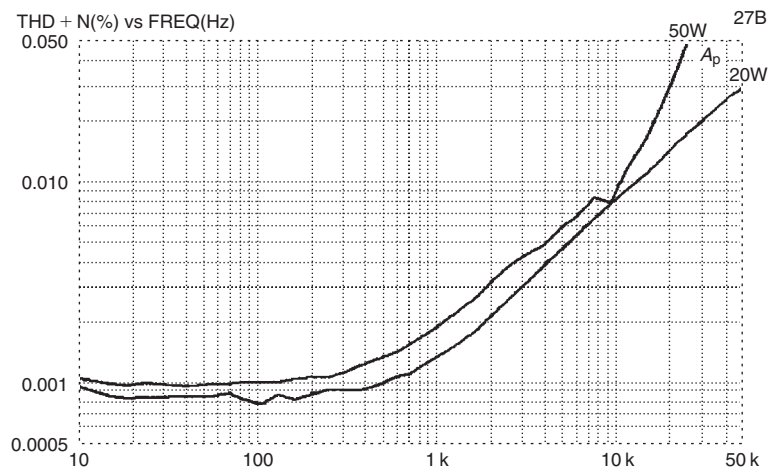


Figure 12.13: THD versus frequency, at 20W (below transition) and 50W into an 8Ω load. The joggle around 8 kHz is due to a cancelation of harmonics from crossover and transition. Bandwidth 80 kHz

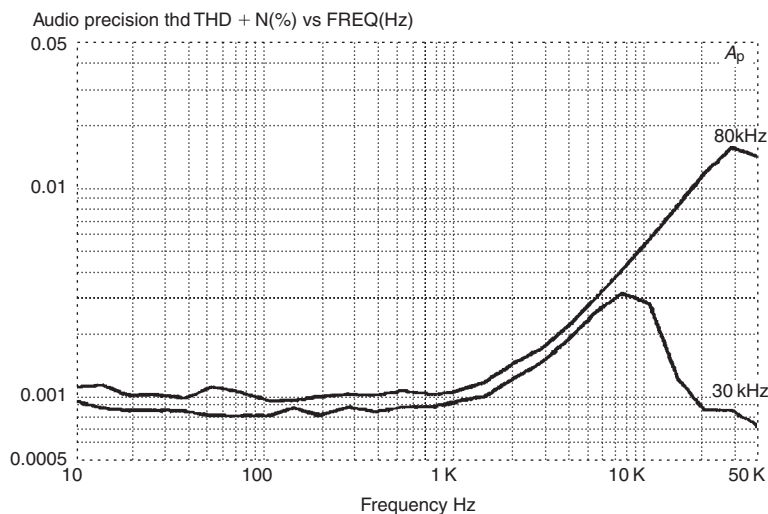


Figure 12.14: THD versus frequency for a Blameless Class-B amplifier at 50W, 8Ω

plot in Figures 12.9 and 12.11. Figure 12.16 confirms that at 20W, below transition, the residual is indistinguishable from that of a Blameless Class-B amplifier; in this region, where the amplifier is likely to spend most of its time, there are no compromises on quality.

Figure 12.17 shows THD versus level, demonstrating how THD increases around 28W as transition begins. The steps at about 10W are nothing to do with the amplifier – they are artefacts due to internal range-switching in the measuring system.

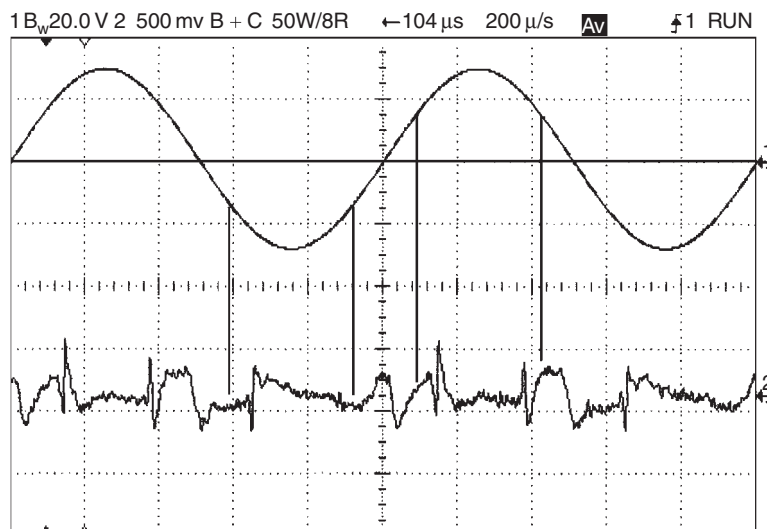


Figure 12.15: The THD residual waveform at 50W into 8Ω. This residual may look rough, but in fact it had to be averaged eight times to dig the glitches and crossover out of the noise; THD is only 0.0012%. The vertical lines show where transition occurs

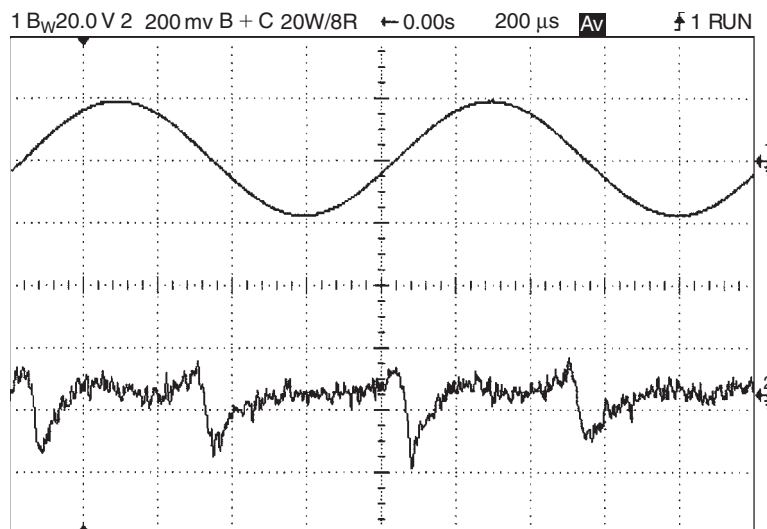


Figure 12.16: The THD residual waveform at 20W into 8Ω, below transition. Only crossover artefacts are visible as there is no rail-switching

Figure 12.18 shows for real the benefits of powering the inner drivers from the outer supply rails. In SPICE simulation (see above) the gain-steps were roughly halved in size by this modification, and Figure 12.18 duly confirms that the THD is halved in the HF region, the only area where it is sufficiently clear of the noise floor to be measured with any confidence.

Deriving a New Kind of Amplifier: Class-A + C

A conventional Class-B power amplifier can be almost instantly converted to push-pull Class-A simply by increasing the bias voltage to make the required quiescent current flow. This is the only real circuit change, though naturally major increases in heat-sinking and power-supply capability are required for practical use. Exactly the same principle applies to the Class-G amplifier. In the book *Self On Audio*^[6] I suggested a new and much more flexible system for classifying amplifier types and here it comes in very handy. Describing Class-G operation as Class-B + C immediately

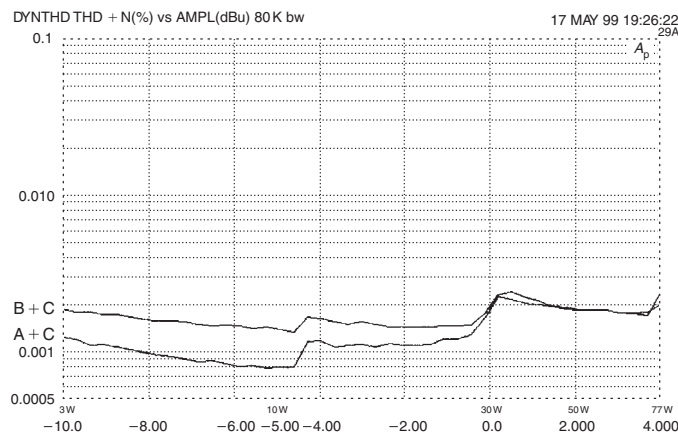


Figure 12.17: THD versus level, showing how THD increases around 28W as transition begins. Class-A + C is the lower and Class-B + C the upper trace

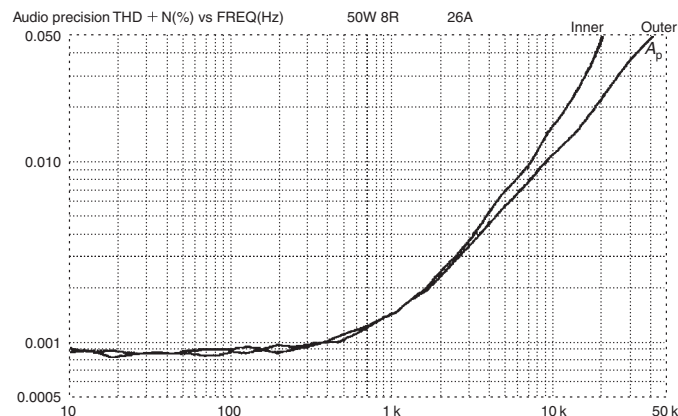


Figure 12.18: THD plot of real amplifier driving 50W into 8Ω. Rails were ± 40 and ± 25 V. Distortion at HF is halved by connecting the inner drivers to the outer supply rails rather than the inner rails